Journal of Crystal Growth 630 (2024) 127602

Contents lists available at ScienceDirect

Journal of Crystal Growth

journal homepage: www.elsevier.com/locate/jcrysgro

Effect of oxygen-related defects on the performance of seed-end wafers in Ga-doped recharged Czochralski silicon: Thermal donors

Jie Huang [a], Ruokai Wu [a], Huali Zhang [c], Chen Wang [c], Dongli Hu [c,d], Shuai Yuan [a,*], Lei Wang [a], Deren Yang [a], Xuegong Yu [a,b,*]

[a] State Key Laboratory of Silicon and Advanced Semiconductor Materials and School of Materials Science and Engineering, Zhejiang University, Hangzhou 310027, PR China
[b] Hangzhou Global Scientific and Technological Innovation Center, Zhejiang University, Hangzhou 311200, PR China
[c] Jiangsu Key Lab of Silicon Based Electronic Materials, Jiangsu GCL Silicon Material Technology Development Co., Ltd., No.88 Yangshan Road, Xuzhou Economic Development Zone, Xuzhou 221000, PR China
[d] School of Materials Science and Engineering, NingboTech University, Ningbo 315100, PR China

ARTICLE INFO

Communicated by Chung wen Lan

Keywords:
A2. Recharged Czochralski silicon
A1. Ga-doped silicon
A1. Thermal donors
B3. Solar cells
A1. FTIR
A1. Minority carrier lifetime

ABSTRACT

Ga-doped recharged Czochralski silicon (Ga-RCZ) is now becoming mainstream in the current photovoltaic market because of the enhanced production efficiency and reduced costs. It also hardly suffers from light-induced degradation (LID) due to the absence of boron-oxygen complexes. However, the performance deterioration of the seed-end wafers universally exists in industrial Ga-RCZ production, even if no ring-like defects are found there. Considering the severe enrichment of oxygen in the seed-end part due to crucible corrosion and oxygen segregation, oxygen-related defects like oxygen precipitates (OPs) and thermal donors (TDs) are easy to generate and may account for this deterioration. In this paper, comprehensive characterization methods including resistivity, minority carrier lifetime (MCL), and Fourier Transform Infrared Spectroscopy (FTIR) were used to identify the true reason for the deterioration in three randomly selected industrial Ga-RCZ ingots with different interstitial oxygen concentrations ($[O_i]$). The results showed that no OPs were observed but TDs were produced even up to 6.87×10^{14} cm^{-3} in the samples. It reveals that TDs should be the culprit for the performance degradation at seed-end wafers in Ga-RCZ.

1. Introduction

RCZ technique has been recently successfully developed based on the traditional production process of Czochralski (CZ) silicon. The characteristic of RCZ technique is that operators can pull more ingots through multiple recharging processes after the first ingot is pulled. Therefore, RCZ could reduce the duration for dismantling the furnace, inflating and deflating the furnace atmosphere, and replacing crucibles, which increases the charging amount of one production circle and reduces the crucible costs, thereby enhancing production efficiency and economic benefits. Ga-doped RCZ not only benefits from the superiority of RCZ technique but also hardly suffers from LID due to the absence of boron-oxygen complexes [1–5], which makes it mainstream in the photovoltaics market. However, the performance deterioration of wafers near the seed end universally exists in industrial Ga-RCZ production, as shown in Fig. 1. Due to the fact that the segregation coefficients of common metal impurities in silicon like Fe, Cu, Ni, and Cr, are much less than 1, this deterioration at seed-end parts is supposed not to be caused by metals. Considering the crucible coating will peel off and the quartz crucible will be damaged by corrosion during the long-time Ga-RCZ production, massive oxygen will infiltrate into silicon and enrich at the seed-end part due to segregation, which is conducive to giving birth to oxygen-related defects, such as OPs and TDs. During the wafer inspection and sorting process, as these wafers exhibiting low lifetime are not considered as a prime grade, it represents a great loss for the wafer manufacturers. Therefore, it is essential to find out which is the true reason for the MCL decline at the seed-end wafers. Some researchers pointed out that OPs usually occur in high-oxygen silicon and should be responsible for the low MCL [6–9]. Basnet et al reported that OPs can also occur during TD formation, resulting in recombination-active ring-like defects through

* Corresponding authors at: State Key Laboratory of Silicon and Advanced Semiconductor Materials and School of Materials Science and Engineering, Zhejiang University, Hangzhou 310027, PR China (X. Yu).
E-mail addresses: shuaiyuan@zju.edu.cn (S. Yuan), yuxuegong@zju.edu.cn (X. Yu).

https://doi.org/10.1016/j.jcrysgro.2024.127602
Received 14 December 2023; Received in revised form 25 January 2024; Accepted 26 January 2024
Available online 28 January 2024

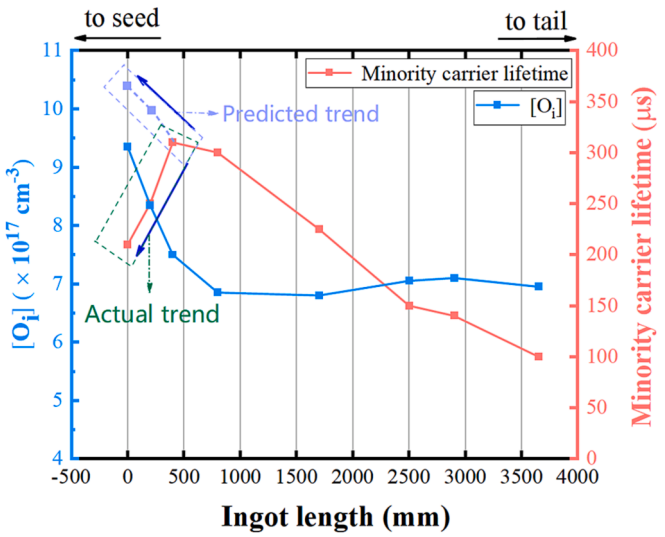

Fig. 1. Performance deterioration universally exists at the seed-end part in the industrial Ga-RCZ silicon (just for example, not the experimental samples). "Predicted trend" refers to the supposed lifetime trend based on metal impurities segregation, while "Actual trend" refers to the real one related to [O_i].

experimental and simulation [10]. Siriwardhana et al also demonstrated that OPs could be formed during TD generation temperature at 450℃ due to enhanced diffusion of oxygen by TDs [11]. However, we did not find any proofs to demonstrate the presence of OPs in the as-grown Ga-RCZ wafers, and ring-like defects were not found there as well, both of which will be discussed in detail in Section 3.1. Apart from OPs, TD is another kind of oxygen-related defect in CZ silicon, derived from the aggregation of oxygen atoms [12–14]. TDs can introduce donor energy levels, releasing electrons to make resistivity increase in Ga-RCZ, and will trap minority carriers to cause low lifetime [17–19]. Therefore, it is reasonable that TDs may be formed near the seed end and cause this deterioration because this part with rather high [O_i] is first pulled and will experience a long-time (usually more than 30 h) preservation under heat conditions for a common 4-meter ingot under the ~ 1.6 mm/min pulling velocity, which is favorable for TD formation [12,15,16].

In this work, we randomly selected three Ga-RCZ ingots with different [O_i] grown in the same furnace and aimed to find out the true reason for the performance deterioration at the seed-end Ga-RCZ wafers. The distribution and variation of [O_i] before and after annealing were measured by FTIR. OPs proofs were collected and analyzed by optical microscope observing after annealing and Secco etching. The concentration of TDs ([TDs]) in samples could be derived from the resistivity variations after heat treatment at 650℃ for 30 min. Low-temperature FTIR was applied to further identify TD absorption bands. MCL were also measured in samples to directly reflect the performance deterioration caused by TDs.

2. Experimental

Three Ga-RCZ ingots with different [O_i] were randomly selected from the production line for investigation. They were grown in one production cycle in the same furnace (SiF160-40C, TDG-MT). More growth information can be found in Table 1. After removing the ingot head and tail, several wafers with a thickness of ~ 2 mm were then cut perpendicularly to the growth direction ⟨001⟩ at different locations from the ingots. Then, samples with a size of ~ 50 mm × 50 mm × 2 mm were cut from the wafer center for further measurement after cleaning and polishing. The schematic diagram is shown in Fig. 2.

Table 1
Growth information of the three Ga-RCZ ingots.

Ingot name	[O_i]	Ingot length (mm)	Ingot diameter (mm)	Sample measurement status
L	Low	2569	254	As-grown or annealed at 650℃ for 30 min
M	Middle	2633	254	
H	High	2773	302	

The [O_i] in the samples was measured at room temperature by using a Bruker IFS66V FTIR with a calibration coefficient of 3.14×10^{17} cm^{-2}. Meanwhile, the infrared absorption bands related to the TDs were inspected by low-temperature FTIR (LT-FTIR) at ~ 10 K with a resolution of 4 cm^{-1}. MCL of the samples was measured by the microwave photoconductance decay equipment (μ-PCD, Semilab WT-2000). Samples were chemically passivated by immersing in diluted hydrofluoric acid (5%) for 10 min before MCL measurement to minimize the impact of surface recombination velocity as much as possible. Resistivity of the samples was tested by the four-probe system (Semilab, IPC-6606). Some wafer samples were observed by an optical microscope (OLYMPUS-MX50) after selective etching. The concentration of TDs ([TDs]) can be derived from the resistivity variation of the samples (p_0 = [Ga]-2[TDs]) before and after a 650 °C thermal treatment in a clean furnace with argon protection for 30 min. Here p_0 is the majority carrier concentration calculated from the value of resistivity, [Ga] is the doping concentration of gallium, and [TDs] is the concentration of TDs.

3. Results and discussion

Table 1 shows the specific growth information of the three Ga-RCZ silicon ingots grown in one production cycle. Ingot length refers to the remained part of the ingot after removing the ingot head and tail, as is shown in Fig. 2. Ingot names abbreviated as L, M, H, represent Low, Middle, and High [O_i] in the following description, respectively. Sample location means the distance from the ingot top (unit. %) in the following texts. As each unit of TD can ionize two units of electrons [20,21], and the 650℃ 30 min annealing process could eliminate almost all TDs [22,23], the initial TD concentration ([TD]) can be derived from the resistivity variation of the samples after the 650 °C 30 min thermal treatment if there are TDs in as-grown samples. All the samples were characterized both in the as-grown state and annealed state to compare the differences in [O_i], resistivity, MCL, and [TD].

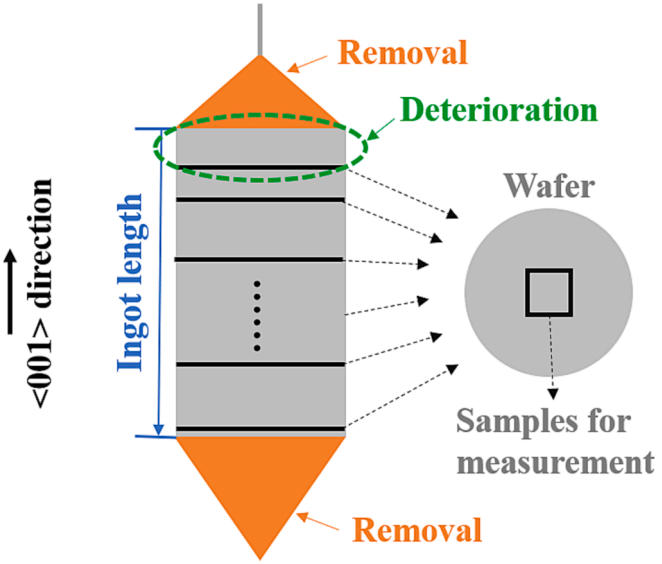

Fig. 2. Schematic diagram of sample processing from the Ga-RCZ ingot body.

3.1. [o_i] distribution

Fig. 3 shows the [O_i] changes at different sample locations after 650℃ 30 min annealing in the three ingots. For the Low-[O_i] and Middle-[O_i] samples, [O_i] first decreases due to segregation, and then increases later possibly due to the additional oxygen released by the quartz crucible whose coating is ruined. Please note that [O_i] hardly changes after annealing in these samples even with different [O_i], while the minor differences in Fig. 3(c) may result from system errors during measurement. The results mean 650℃ 30 min heat treatment would not produce or eliminate OPs, or else [O_i] will change due to oxygen atom precipitating or releasing, respectively. Literature also reported that low-temperature and short-time heat treatment will not have a significant effect on OPs [24], which directly corresponds to the results. Generally speaking, larger-size OPs in silicon can be identified in optical photos after etching. However, no etching patterns of OPs were observed in the optical photos in the samples, as shown in Fig. 3(d). In addition, a high-temperature annealing process (e.g., at ~ 1200℃ for 2 h) could dissolve OPs and contribute to some changes of [O_i] [25,26], which can better clarify small-size OPs. Nevertheless, no significant changes in [O_i] were observed in these samples after this thermal process (not shown here). Moreover, all samples from the three ingots were identified without ring-like defects that were confirmed to relate to OPs in photoluminescence images [27], which further proves there exist no OPs in the as-grown samples. Therefore, the interference of OPs in this study should be ignored accordingly. More results and discussions were focused on TDs in the next.

3.2. Resistivity and MCL

In the low-[O_i] ingot, as plotted in Fig. 4(a) and Fig. 4(d), resistivity and MCL both decrease from the ingot head to the tail, which should be due to the segregation of Ga dopant and the gradual enrichment of harmful metal impurities, respectively. It is noteworthy that resistivity and MCL both remain original values after 650℃ 30 min annealing for all samples in the low-[O_i] ingot ($[O_i]_{max} \leq 6.73 \times 10^{17}cm^{-3}$ plotted in Fig. 3(a)), which can be inferred that TD in the samples hardly exists and thus has little influence on wafer performance. However, in the middle-[O_i] ingot in Fig. 4(b), resistivity decreases from 0.85 Ω·cm to 0.80 Ω·cm after annealing only at the ingot head (named sample-M1 in Table 2) of which [O_i] reaches $7.67 \times 10^{17}cm^{-3}$ (can be found in Fig. 3(b)), while the resistivity of other samples with lower [O_i] hardly changes. Thus, [TD] can be obtained as $4.79 \times 10^{14}cm^{-3}$ according to the resistivity drifts at $[O_i] = 7.67 \times 10^{17}cm^{-3}$ at the ingot head (sample-M1) in the middle-[O_i] ingot, and the results are summarized in Table 2. Correspondingly, MCL obviously increases for the annealed sample at the ingot head, as shown in Fig. 4(e), which is inferred that the as-grown TDs are responsible for the performance deterioration and the annealing process benefits to reduce the impact of TDs on wafer's performance. As for the high-[O_i] ingot ($[O_i]_{min} \geq 7.02 \times 10^{17}cm^{-3}$ plotted in Fig. 3(c)),

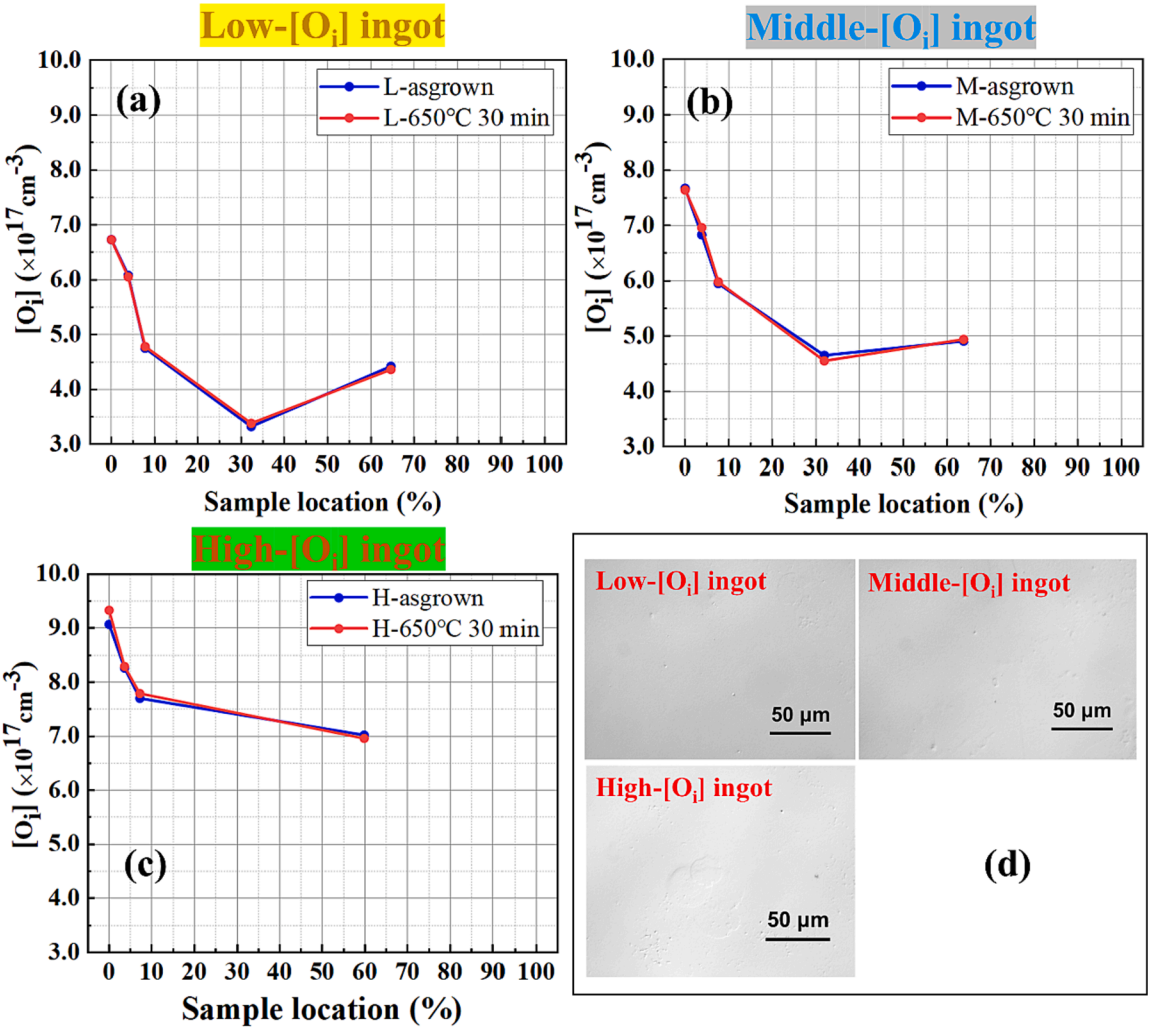

Fig. 3. Interstitial oxygen concentration [O_i] at different sample locations in the low-[O_i] ingot (**a**), middle-[O_i] ingot (**b**), and high-[O_i] ingot (**c**), respectively. (**d**) Optical photos of wafers after Secco etching.

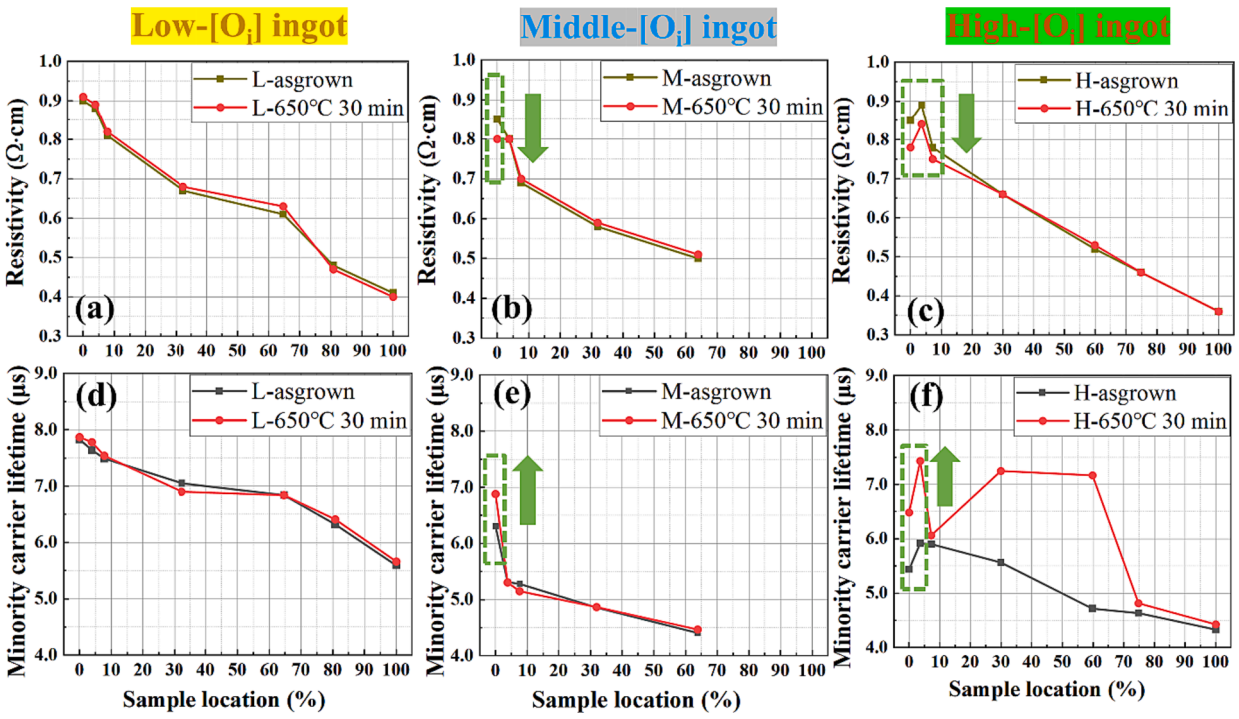

Fig. 4. (**a-c**) Resistivity at different sample locations in the three ingots. (**d-f**) MCL at different sample locations in the three ingots.

Table 2
Summary of [TD] and [O_i] at the head samples in the three ingots.

Sample name	[O_i]	[TD]	Ingot name	Sample location
L	$\leq 6.73 \times 10^{17}$ cm^{-3}	0	L	All locations
M1	7.67×10^{17} cm^{-3}	4.79×10^{14} cm^{-3}	M	0
H1	9.07×10^{17} cm^{-3}	6.87×10^{14} cm^{-3}	H	0
H2	8.26×10^{17} cm^{-3}	4.35×10^{14} cm^{-3}	H	3.6%
H3	7.70×10^{17} cm^{-3}	3.34×10^{14} cm^{-3}	H	7.2%

[TD] at the seed-end part (sample locations are 0%, 3.6%, and 7.2%, with [O_i] $\geq 7.70 \times 10^{17} cm^{-3}$) can also be derived from the resistivity drifts after annealing, and the results (sample-H1, sample-H2, and sample-H3) are also summarized in Table 2. After annealing, MCL of these samples around the ingot head increases because of the elimination of TDs. However, MCL of other samples at the middle or tail in the high-[O_i] ingot body is abnormally sharply raised, as circled in Fig. 4(f). This is obviously unrelated to TDs because the [TDs] is calculated as zero based on resistivity variations and the reason remains unclear to us. We supposed it may be caused by the instrument errors during sample measurement.

Table 2 summarizes the above results and shows some relations between [O_i] and [TD]. In addition, the relation between [TD] and heat duration (i.e., thermal history) is also discussed here. On one hand, TD derives from the aggregation of oxygen atoms, which means higher [Oi] helps to generate more TDs. On the other hand, sample locations can represent different heat durations before the ingots cool to room temperature, so the first-pulled samples will experience a longer duration, and this is also beneficial for producing more TDs [28]. In the same one high-[Oi] ingot, [Oi] and heat durations are both: sample-H1 > sample-H2 > sample-H3, so [TD] gradually decreases from sample-H1 to sample-H3. But for the sample-M1 with [O_i] = 7.67×10^{17} cm^{-3} in the middle-[O_i] ingot, its [TD] seems higher than sample-H2 with [O_i] = 8.26×10^{17} cm^{-3} and sample-H3 with [O_i] = 7.70×10^{17} cm^{-3} in the high-[Oi] ingot, and this may because sample-M1 has a longer duration due to different locations. In the same one low-[O_i] ingot, even if the seed-end samples had the longest duration and highest [O_i] than other location samples, [TD] is still too small to count, which reminds manufacturers should try to control [O_i] below this value when having the same thermal history as the low-[Oi] ingot to avoid TDs during the production process.

3.3. LT-FTIR spectra

Fig. 5 shows the LT-FTIR spectrums of samples with different [O_i]. Several peaks of TD families (i.e., TD1, TD3, TD4, TD6, TD7, TD9) and O_i peak are marked according to literature reports [20,29–31]. From the results, we can observe that the peak position and intensity of O_i keep unchanged after annealing, which means few oxygen-related complexes or precipitates are formed during the annealing. Only TD6 at ~ 417 cm^{-1} and TD7 at ~ 791 cm^{-1}, circled by black dotted rectangular in the figures, seem to be the main factors that lead to resistivity drift and performance degradation in the samples, as they are [O_i]-related (when [O_i] is less than $6.73 \times 10^{17} cm^{-3}$, they do not exist.) and can be thoroughly eliminated by 650°C 30 min annealing, which is consistent with the common electrically-active TD features. Other families do not possess the above characteristics but seem to undergo configuration transitions after the annealing such as from TD9 at ~ 559 cm^{-1} to TD1 ~ 507 cm^{-1}, because the absorbance intensities of TD1 and TD9 partly changed possibly due to the decomposition and re-aggregation of oxygen clusters during the annealing in some samples, which could be related to the formation of new donors.

In general, TD is usually considered as shallow donors. Until now, researchers have shown that there are at least 16 different families of TDs (TD1 ~ TD16) [31–33], and their energy levels are basically located at about E_c-0.05 eV and E_c-0.15 eV [34,35]. Li et al. used deep level transient spectroscopy (DLTS) measurements to demonstrate that the introduced TDs can cause an energy level at Ec-0.13 eV with carrier capture cross-section of 10^{-15} cm^2, which can significantly reduce the

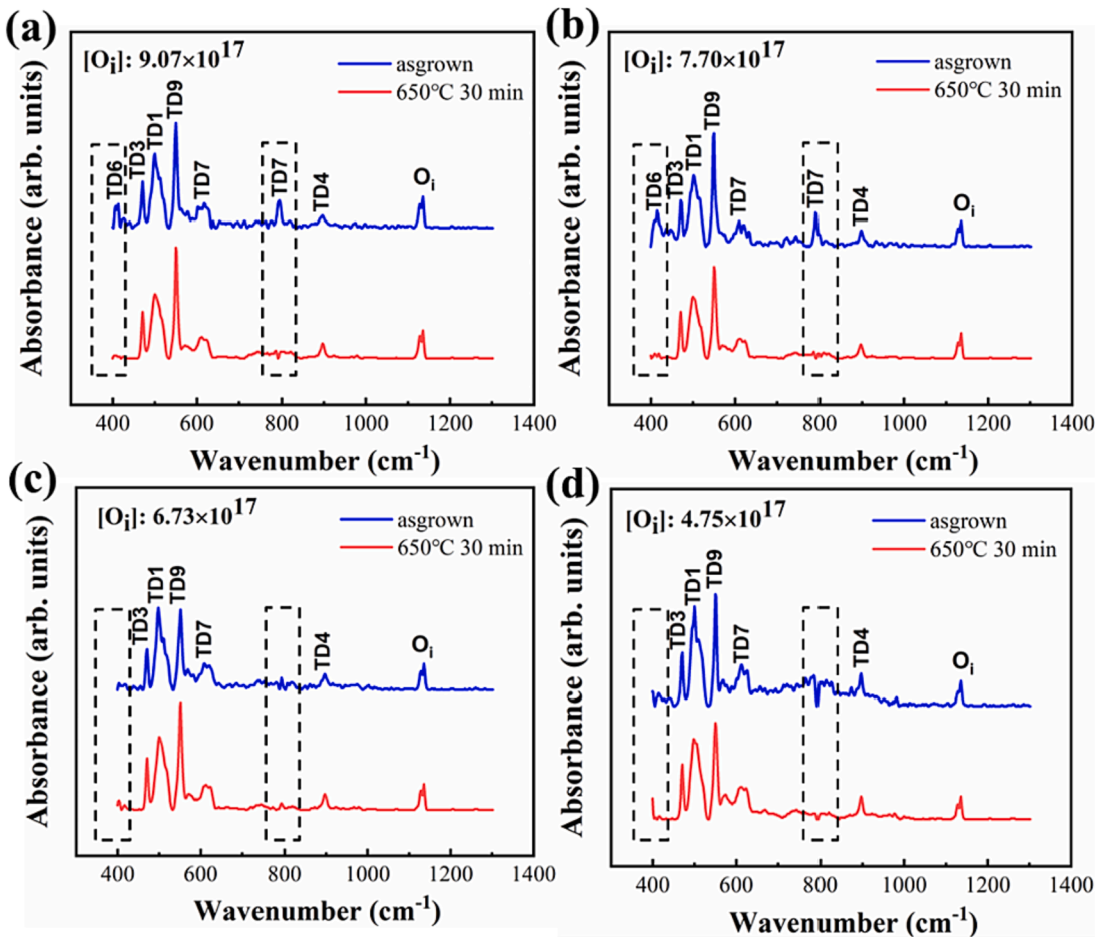

Fig. 5. LT-FTIR spectrums of samples with different [O_i]: (**a**) 9.07 × 10^{17}cm^{-3} (**b**) 7.77 × 10^{17}cm^{-3} (**c**) 6.73 × 10^{17}cm^{-3} (**d**) 4.75 × 10^{17}cm^{-3} before and after annealing at 650 ℃ for 30 min. Measurement temperature: 10 K. Resolution: 4 cm^{-1}.

carrier lifetime of n-type silicon substrate in silicon heterojunction solar cells [17]. Tomassini et al. found a deep energy level in the range of 0.2–0.3 eV below the conduction band that limits the carrier lifetime, and that the second family of TDs, featuring bistable properties, was tentatively identified as the corresponding defect that leads to unacceptable efficiency losses, greater than 1% absolute, in heterojunction solar cells [19].

Generally speaking, TDs can be eliminated by a single 650℃ 30 min annealing process or during cell fabrication with high-temperature procedures like phosphorus/boron diffusion, gettering, and sintering, but the TD-contained as-grown wafers that exhibit low lifetime are not considered as a prime grade for sale during the wafer inspection and sorting process before cell fabrication, which represents a great loss for the silicon wafer manufacturers. For this reason, wafer manufacturers should take some methods to reduce the impact of TDs on the as-grown wafer performance and economic benefits, such as reducing oxygen content and avoiding staying in the TD-produced-friendly temperature range for too long.

4. Conclusion

Ga-RCZ is becoming mainstream in the photovoltaics market, however, the performance deterioration of seed-end wafers universally exists in industrial Ga-RCZ production, which reduces economic benefits and limits its development. Through investigating and analyzing the variations of sample parameters including [O_i], resistivity, and MCL in three asgrown ingots before and after the 650℃ 30 min annealing process, TDs are revealed to exist at the seed-end wafers and cause resistivity drift and MCL decline rather than our conventional perception of OPs. TD concentration is related to both oxygen and heating duration, which reminds wafer manufacturers to take some economical and feasible methods to relieve the TDs influence by adjusting crystal growth processes and reducing the oxygen content.

Declarations

This manuscript is the authors' original work and has not been published nor submitted simultaneously elsewhere.

CRediT authorship contribution statement

Jie Huang: Writing – review & editing, Writing – original draft, Methodology, Investigation, Formal analysis, Data curation, Conceptualization. **Ruokai Wu:** Formal analysis. **Huali Zhang:** Resources, Funding acquisition, Conceptualization. **Chen Wang:** Resources, Project administration, Funding acquisition, Conceptualization. **Dongli Hu:** Resources. **Shuai Yuan:** Supervision, Resources, Funding acquisition. **Lei Wang:** Supervision, Resources, Project administration, Funding acquisition. **Deren Yang:** Supervision, Resources, Project administration, Funding acquisition. **Xuegong Yu:** Writing – review & editing, Supervision, Funding acquisition.

Declaration of Competing Interest

The authors declare that they have no known competing financial interests or personal relationships that could have appeared to influence the work reported in this paper.

Data availability

All data generated or analyzed during this study are included in this published article [and its supplementary information files].

Acknowledgements

The authors would like to thank Qi Zhang at Jiangsu GCL Silicon Material Technology Development Co., Ltd., for sample fabrication and delivery.

Funding

This work was supported by the National Natural Science Foundation of China [Nos. 62025403, U23A20354 and 62004173]; the Natural Science Foundation of Zhejiang Province [LD22E020001 and LDQ23E020002]; the Inner Mongolia Autonomous Region Science and Technology Plan Project (2023JBGS0017), "Pioneer" and "Leading Goose" R&D Program of Zhejiang [2022C01215]; the Fundamental Research Funds for the Central Universities [226-2022-00200]; the Open Project of Jiangsu Provincial Key Laboratory of Silicon-based Electronic Materials; and the Open Project of Key Laboratory of Solar Energy Utilization and Energy Saving technology of Zhejiang Province [No. ZJS-OP-2020-01].

References

[1] R. Basnet, C. Sun, T. Le, Z. Yang, A. Liu, Q. Jin, Y. Wang, D. Macdonald, Investigating Wafer Quality in Industrial Czochralski-Grown Gallium-Doped p-Type Silicon Ingots with Melt Recharging, Sol. RRL 7 (2023) 2300304, https://doi.org/10.1002/solr.202300304.

[2] B. Lim, K. Bothe, J. Schmidt, Deactivation of the boron–oxygen recombination center in silicon by illumination at elevated temperature, Phys Status Solidi Rapid Res Lett 3 (2008) 93–95, https://doi.org/10.1002/pssr.200802009.

[3] D. Macdonald, F. Rougieux, A. Cuevas, B. Lim, J. Schmidt, M.D. Sabatino, L. J. Geerligs, Light-induced boron-oxygen defect generation in compensated p-type Czochralski silicon, J. Appl. Phys. 105 (2009) 093704, https://doi.org/10.1063/1.3121208.

[4] A. Herguth, G. Schubert, M. Kaes, G. Hahn, Investigations on the long time behavior of the metastable boron–oxygen complex in crystalline silicon, Prog. Photovolt: Res. Appl. 16 (2008) 135–140, https://doi.org/10.1002/pip.779.

[5] B. Lim, S. Hermann, K. Bothe, J. Schmidt, R. Brendel, Solar cells on low-resistivity boron-doped Czochralski-grown silicon with stabilized efficiencies of 20%, Appl. Phys. Lett. 93 (2008) 162102 https://doi.org/10.1063/1.3003871.

[6] K. Kinoshita, T. Kojima, K. Onishi, Y. Ohshita, A. Ogura, Effect of oxygen precipitation through annealing process on lifetime degradation by Czochralski-Si crystal growth conditions, Jpn. J. Appl. Phys. 58 (2019) SBBF02, https://doi.org/10.7567/1347-4065/aaf87b.

[7] L. Chen, X. Yu, P. Chen, P. Wang, X. Gu, J. Lu, D. Yang, Effect of oxygen precipitation on the performance of Czochralski silicon solar cells, Sol. Energy Mater Sol. Cells 95 (2011) 3148–3151, https://doi.org/10.1016/j.solmat.2011.06.044.

[8] J.D. Murphy, M. Al-Amin, K. Bothe, M. Olmo, V.V. Voronkov, R.J. Falster, The effect of oxide precipitates on minority carrier lifetime in n-type silicon, J. Appl. Phys. 118 (2015) 215706, https://doi.org/10.1063/1.4936852.

[9] J.D. Murphy, K. Bothe, M. Olmo, V.V. Voronkov, R.J. Falster, The effect of oxide precipitates on minority carrier lifetime in p-type silicon, J. Appl. Phys. 110 (2011) 053713, https://doi.org/10.1063/1.3632067.

[10] R. Basnet, H. Sio, M. Siriwardhana, F. Rougieux, D. Macdonald, Ring-Like Defect Formation in N-Type Czochralski-Grown Silicon Wafers during Thermal Donor Formation, Phys. Status Solidi A 218 (2021) 2000587, https://doi.org/10.1002/pssa.202000587.

[11] M. Siriwardhana, F. Rougieux, R. Basnet, H. Nguyen, D. Macdonald, Photoluminescence Spectroscopy of Thermal Donors and Oxygen Precipitates Formed in Czochralski Silicon at 450 °C, IEEE J. Photovoltaics 12 (2022) 222–229, https://doi.org/10.1109/JPHOTOV.2021.3126120.

[12] W. Kaiser, H.L. Frisch, H. Reiss, Mechanism of the Formation of Donor States in Heat-Treated Silicon, Phys. Rev. 112 (1958) 1546, https://doi.org/10.1103/PhysRev.112.1546.

[13] N. Meilwes, J.-M. Spaeth, V.V. Emstev, G.A. Oganesyan, On the nature and structures of different heat treatment centres in n- and p-type silicon, Sci. Technol. 9 (1994) 1346–1353, https://doi.org/10.1088/0268-1242/9/7/008.

[14] A. Ourmazd, W. Schröter, A. Bourret, Oxygen-related thermal donors in silicon: A new structural and kinetic model, J. Appl. Phys. 56 (1984) 1670–1681, https://doi.org/10.1063/1.334156.

[15] M. Clayboum, R.C. Newman, Thermal donor formation and the loss of oxygen from solution in silicon heated at 450 °C, Appl. Phys. Lett. 52 (1988) 2139–2141, https://doi.org/10.1063/1.99557.

[16] K. Torigoe, T. Ono, Formation of thermal donor enhanced by oxygen precipitation in silicon crystal, AIP Advances 10 (2020) 045019, https://doi.org/10.1063/1.5140206.

[17] J. Li, X. Yu, S. Yuan, L. Yang, Z. Liu, D. Yang, Effects of oxygen related thermal donors on the performance of silicon heterojunction solar cells, Sol. Energy Mater Sol. Cells 179 (2018) 17–21, https://doi.org/10.1016/j.solmat.2018.02.006.

[18] V.P. Markevich, M. Vaqueiro-Contreras, S.B. Lastovskii, L.I. Murin, M.P. Halsall, A. R. Peaker, Electron emission and capture by oxygen-related bistable thermal double donors in silicon studied with junction capacitance techniques, J. Appl. Phys. 124 (2018) 225703, https://doi.org/10.1063/1.5053805.

[19] M. Tomassini, J. Veirman, R. Varache, E. Letty, S. Dubois, Y. Hu, Ø. Nielsen, Recombination activity associated with thermal donor generation in monocrystalline silicon and effect on the conversion efficiency of heterojunction solar cells, J. Appl. Phys. 119 (2016) 084508, https://doi.org/10.1063/1.4942212.

[20] D. Wruck, P. Gaworzewski, Electrical and infrared spectroscopic investigations of oxygen-related donors in silicon, Phys. Status Solidi A 56 (1979) 557–564, https://doi.org/10.1002/pssa.2210560220.

[21] A.R. Bean, R.C. Newman, The effect of carbon on thermal donor formation in heat treated pulled silicon crystals, J. Phys. Chem. Solids 33 (1972) 255–268, https://doi.org/10.1016/0022-3697(72)90004-2.

[22] Y. Tokuda, N. Kobayashi, A. Usami, Y. Inoue, M. Imura, Thermal donor annihilation and defect production in ntype silicon by rapid thermal annealing, J. Appl. Phys. 66 (1989) 3651–3655, https://doi.org/10.1063/1.344076.

[23] E. Olsen, T. Mehl, H.E. Stalheim, M. Juel, R. Søndenå, I. Burud, The Effect of Pull Speed and Heat Treatment on Thermal Donors in Czhocralski Silicon, Phys. Status Solidi A 219 (2022) 2100655, https://doi.org/10.1002/pssa.202100655.

[24] A. Borghesi, B. Pivac, A. Sassella, A. Stella, Oxygen precipitation in silicon, J. Appl. Phys. 77 (1995) 4169–4244, https://doi.org/10.1063/1.359479.

[25] I. Yonenaga, K. Sumino, Mechanical Behavior of Czochralski-Silicon Crystals as Affected by Precipitation and Dissolution of Oxygen Atoms, Jpn. J. Appl. Phys. 21 (1982) 47–55, https://doi.org/10.1143/JJAP.21.47.

[26] Z. Wang, X. Yu, S. Yuan, D. Yang, Electrical properties of oxygen precipitate-related defects in Czochralski silicon, Appl. Phys. Express 15 (2022) 071004. https://doi.org/10.35848/1882-0786/ac7432.

[27] Z. Wang, X. Zhu, S. Yuan, X. Yu, D. Yang, Comprehensive characterization of efficiency limiting defects in the swirl-shaped region of Czochralski silicon, Sol. Energy Mater Sol. Cells 236 (2022) 111533, https://doi.org/10.1016/j.solmat.2021.111533.

[28] Y. Kamiura, F. Hashimoto, M. Yoneta, Generation of several kinds of oxygen-related thermal donors around 520 °C in Czochralski silicon, J. Appl. Phys. 66 (1989) 3926–13029, https://doi.org/10.1063/1.344018.

[29] P. Wagner, J. Hage, Thermal double donors in silicon, Appl. Phys. A 49 (1989) 123–138. https://link.springer.com/article/10.1007/BF00616290.

[30] C. Cui, D. Yang, X. Ma, M. Li, D. Que, Effect of light germanium doping on thermal donors in Czochralski silicon wafers, Mater. Sci. Semicond. Process. 9 (2006) 110–113, https://doi.org/10.1016/j.mssp.2006.01.034.

[31] J.L. Lindström, T. Hallberg, Vibrational infrared-absorption bands related to the thermal donors in silicon, J. Appl. Phys. 77 (1995) 2684–2690, https://doi.org/10.1063/1.358736.

[32] W. Götz, G. Pensl, W. Zulehner, Observation of five additional thermal donor species TD12 to TD16 and of regrowth of thermal donors at initial stages of the new oxygen donor formation in Czochralski-grown silicon, Phys. Rev. B 46 (1992) 4312, https://doi.org/10.1103/PhysRevB.46.4312.

[33] T. Hallberg, J.L. Lindström, Infrared vibrational bands related to the thermal donors in silicon, J. Appl. Phys. 79 (1996) 7570–7581, https://doi.org/10.1063/1.362413.

[34] H.J. Hoffmann, H. Nakayama, T. Nishino, Y. Hamakawa, Differential evaluation of the Hall effect in silicon with oxygen-related donors, Appl. Phys. A 33 (1984) 47–50, https://doi.org/10.1007/BF01197085.

[35] M. Bruzzia, D. Menichelli, M. Scaringella, Thermal donors formation via isothermal annealing in magnetic Czochralski high resistivity silicon, J. Appl. Phys. 99 (2006) 093706, https://doi.org/10.1063/1.2192307.